Published in Plant Physiology, Vol. 162, Issue 2, 2013, p. 652-662
which should be used for any reference to this work

A Chloroplast ABC1-like Kinase Regulates Vitamin E Metabolism in Arabidopsis[1][C][W][OA]

Jacopo Martinis, Gaétan Glauser, Sergiu Valimareanu, and Felix Kessler*

Laboratory of Plant Physiology (J.M., S.V., F.K.) and Chemical Analytical Service of the Swiss Plant Science Web (G.G.). University of Neuchâtel, 2000 Neuchâtel, Switzerland

In bacteria and mitochondria, ABC1 (for Activity of bc1 complex)-like kinases regulate ubiquinone synthesis, mutations causing severe respiration defects, including neurological disorders in humans. Little is known about plant ABC1-like kinases; in Arabidopsis (*Arabidopsis thaliana*), five are predicted in mitochondria but, surprisingly, six are located at lipid droplets in chloroplasts. These are a known site of prenylquinone (including tocopherol [vitamin E], phylloquinone [vitamin K] and plastoquinone) metabolism and contain a large proportion of the tocopherol cyclase (VTE1) required for vitamin E synthesis and recycling. Therefore, ABC1-like kinases may be involved in the regulation of chloroplast prenylquinone metabolism. Using a nontargeted lipidomics approach, we demonstrate that plants lacking the plastoglobule ABC1-like kinase ABC1K3 are defective both for the production of plastochromanol-8 (a plastoquinone-derived lipid antioxidant) and the redox recycling of α-tocopherol, whereas tocopherol production is not affected. All of these pathways require VTE1 activity. However, in the *abc1k3* mutant, VTE1 levels are strongly reduced posttranscriptionally. We provide evidence that the ABC1-like kinase ABC1K3 phosphorylates VTE1, possibly stabilizing it at plastoglobules. However, ABC1K3 may also have other targets and be involved in a wider chloroplast regulatory network.

Prenylquinones make up a class of lipophilic molecules that includes essential electron carriers in bacterial respiration, mitochondria and chloroplasts (ubiquinone, plastoquinone, and phylloquinone), and compounds with physiological antioxidant activity (tocopherols, tocotrienols, and plastochromanol), some of which (tocopherol [vitamin E] and phylloquinone [vitamin K]) are required as vitamins in human nutrition (Bouvier et al., 2005; Mène-Saffrané and DellaPenna, 2010). The key enzymes involved in prenylquinone biosynthesis are mostly known, but the regulation of the pathways is still poorly understood. Members of the ABC1/ADCK/UbiB (for Activity of bc1 complex/ABC1 domain containing kinase/ubiquinone biosynthesis protein B) family of atypical kinases are candidates for such regulators. The ABC1/ADCK/UbiB family consists of putative kinases, identified by sequence alignment methods (Psi-BLAST and hidden Markov models), that have a domain similar to the eukaryotic protein kinase domain. This includes the most conserved metal binding residues and catalytic motifs. Members of the ABC1 family were found both in bacteria and eukaryotes. These findings suggest that the family evolved in bacteria and entered early eukaryotes by horizontal transfer (Leonard et al., 1998). The prototypical family member, yeast (*Saccharomyces cerevisiae*) ABC1, is defective in aerobic respiration because of a reduction in mitochondrial ABC1. The defect can be overcome by exogenously supplied decylubiquinol (Bousquet et al., 1991; Brasseur et al., 1997). Similarly, mutations of the human ABC1 homolog (CABC1 [for chaperone activity of bc1 complex] or ADCK3) cause ubiquinone deficiency and defects in the respiratory chain, resulting in a progressive neurological disorder with cerebellar atrophy, developmental delay, and hyperlactatemia (Mollet et al., 2008). Studies performed on bacteria showed that *YigR*, the *Escherichia coli* homolog of *ABC1*, corresponds to *UbiB*, a gene required for the first monooxygenase step in ubiquinone biosynthesis (Poon et al., 2000). Prior experiments identified a pool of octaprenylphenol that remained bound to a protein complex until it was activated in the presence of oxygen to continue the ring modifications required in ubiquinone biosynthesis (Knoell, 1981). The rapid conversion of octaprenylphenol to Ubiquinone-8 upon transfer from anaerobic to aerobic growth conditions is consistent with a mechanism that may require kinase regulation. Moreover, ABC1 has been shown to be able to complement the yeast mutant *coenzyme Q biosynthesis mutant 8, accession 1*, defective in ubiquinone synthesis (Do et al., 2001). Despite its widely accepted role in ubiquinone synthesis, little is known about the

[1] This work was supported by the Swiss Plant Science Web (to G.G.), by the University of Neuchâtel, SystemsX Plant Growth in a Changing Environment, National Centre of Competence in Research Plant Survival and the Swiss National Science Foundation (grant no. 31003A–127380 to F.K.), and by Sciex (grant no. 12.095 to S.V.).

* Corresponding author; e-mail felix.kessler@unine.ch.

The author responsible for distribution of materials integral to the findings presented in this article in accordance with the policy described in the Instructions for Authors (www.plantphysiol.org) is: Felix Kessler (felix.kessler@unine.ch).

[C] Some figures in this article are displayed in color online but in black and white in the print edition.

[W] The online version of this article contains Web-only data.

[OA] Open Access articles can be viewed online without a subscription.

exact function and the in vivo targets of ABC1. In yeast, it has been demonstrated that Coq3, Coq5, and Coq7 polypeptides are phosphorylated in an ABC1/Coq8-dependent manner and that the expression of the human homolog ADCK3/CABC1 rescued the growth of yeast *coq8* mutants as well as the phosphorylation state of several of the Coq polypeptides, suggesting the existence of multiple enzyme targets of the kinase in the ubiquinone biosynthesis pathway (Xie et al., 2011).

Until recently, ABC1-like kinases have been mainly studied in mitochondria and bacteria, while little evidence was obtained on the role of their chloroplast homologs. One of these putative kinases, AtOSA1 (for Arabidopsis [*Arabidopsis thaliana*] Oxidative Stress-related ABC1-like protein) was identified in the inner envelope membrane of Arabidopsis chloroplasts (Jasinski et al., 2008). The analysis of gene expression showed that *AtOSA1* transcription is induced by Cd^{2+} treatment and oxidative stress conditions, and knockout plants for this gene permanently suffer from oxidative stress. However, AtOSA1 was unable to complement yeast strains lacking the endogenous *ABC1* gene, and this suggests a different function for this chloroplast kinase when compared with mitochondrial ABC1. Another chloroplast ABC1-like kinase, AtACDO1 (for ABC1-like kinase related to chlorophyll degradation and oxidative stress), has been recently associated with defects in chlorophyll degradation and oxidative stress response under high light conditions (Yang et al., 2012). The *Chlamydomonas reinhardtii* Ser/Thr protein kinase EYEspot assembly mutant 3, belonging to the ABC1 family, has been recently demonstrated to localize to the pigment granule arrays in the eyespot apparatus and to be required for their assembly (Boyd et al., 2011). These carotenoid-filled globules are necessary for the correct assembly of the eyespot complex and are related to chloroplast lipid droplets (plastoglobules; Kreimer, 2009). Plastoglobules are associated with thylakoid membranes (Bréhélin and Kessler, 2008) and known to accumulate carotenoids and prenylquinones (Steinmuller and Tevini, 1985; Deruère et al., 1994). Interestingly, six out of the eight ABC1-like kinases currently identified in Arabidopsis chloroplasts were identified in the proteome of highly purified plastoglobules in several independent studies (Vidi et al., 2006; Ytterberg et al., 2006; Lundquist et al., 2012a, 2012b). Considering the coincident presence of several enzymes involved in prenylquinone metabolism in plastoglobules, it appears possible that the ABC1-like kinases are involved in the regulation of prenylquinone metabolism comparable to ABC1 in the bacterial and mitochondrial ubiquinone pathways.

In this study, we focused on the ABC1-like kinase family member ABC1K3 and its influence on chloroplast prenylquinone composition. ABC1K3 is known to be highly enriched in chloroplast plastoglobules (Vidi et al., 2006; Ytterberg et al., 2006; Lundquist et al., 2012b). Moreover, gene coexpression analysis has recently demonstrated that this kinase clusters together with plastoglobule proteins predicted to be involved in carotenoid metabolism and plastid proteolysis, thus suggesting that ABC1K3 is functionally linked to genes involved in diverse aspects of chloroplast and plastoglobule metabolism (Lundquist et al., 2012b).

RESULTS

Isolation of *ABC1K3* Mutants

In the Salk Institute Genomic Analysis Laboratory (SALK) database, two independent transfer DNA (T-DNA) insertion mutant lines (SALK_128696 and SAIL_918E10) were identified for *ABC1K3* (Alonso et al., 2003), and homozygous plants were selected by PCR genotyping (Supplemental Fig. S1, A–C). The visual phenotype and protein patterns, as well as photosynthetic parameters and lipid composition of the two mutants, were identical (Supplemental Fig. S2, A–C). For these reasons, only the *abc1k3* mutant line SALK_128696 was used for further experiments.

Moreover, a quantitative reverse transcription PCR (RT-PCR) analysis was carried out on total RNA extracted from fresh wild-type and *abc1k3* leaves. No *ABC1K3* transcript was detected in *abc1k3*, demonstrating that it corresponds to a null mutant (Supplemental Fig. S1D).

Nonphotochemical Quenching Is Moderately Affected in the *abc1k3* Mutant under High Light Intensity Treatment

Chlorophyll fluorescence measurements using a Mini-PAM device indicate photosynthetic functions and were carried out on *abc1k3* and tocopherol cyclase (*vte1*) mutants using wild-type plants (ecotype Columbia-0) as the control. The fluorometric determination of the photosynthetic parameters was performed at intervals of 24 h on leaves ($n = 5$) from rosettes grown either under normal light conditions (150 μE m^{-2} s^{-1}) or exposed to continuous high light intensity (HL; 500 μE m^{-2} s^{-1}) for a total duration of 7 d. No significant differences in Photosystem II (PSII) quantum efficiency (*Fv/Fm* [for maximum photochemical efficiency of PSII in the dark-adapted state]) or total electron transport rate (ETR; not shown) were detected between the three plants lines either under normal light intensity or after short HL treatment. A significant reduction in PSII efficiency was observed in the *vte1* mutant starting from 4 d of continuous HL exposure (Fig. 1A). Nonphotochemical quenching (NPQ) in *abc1k3* was slightly lower than in the wild type. In *vte1*, NPQ levels were higher than in wild-type plants after a short exposure (1–3 d) to continuous HL but they significantly decreased under prolonged HL treatment (Fig. 1B).

abc1k3 Mutation Affects Chloroplast Ultrastructure

Transmission electron microscopy was used to analyze the chloroplast ultrastructure in *abc1k3* plants

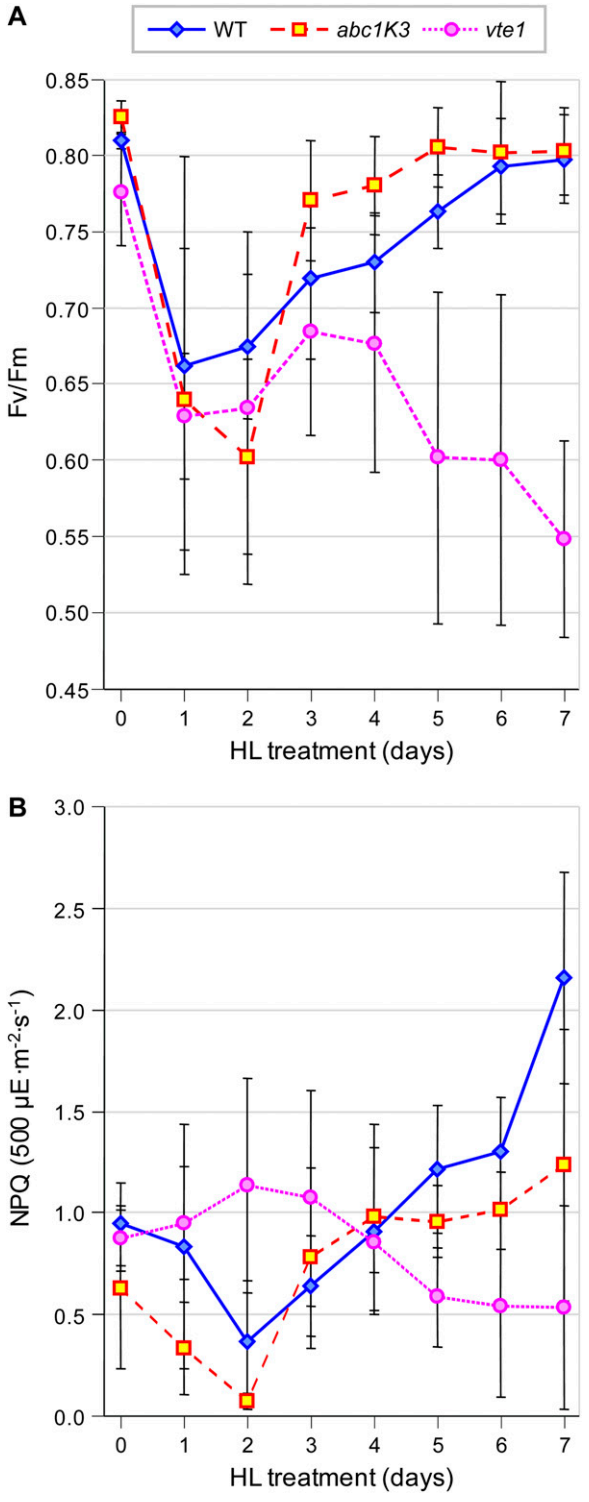

Figure 1. Effect of continuous HL exposure on plant photosynthetic parameters. A, PSII activity (*Fv/Fm*). B, NPQ. Leaves (n = 5) from plants exposed to normal (150 μE m^{-2} s^{-1}) or high (500 μE m^{-2} s^{-1}) light intensity were analyzed at intervals of 24 h. WT, Wild type. [See online article for color version of this figure.]

and compare it with both the wild type and the *vte1* mutant (Fig. 2, A–C). Leaf sections from plants grown under different light intensities were analyzed. Under normal light conditions, *abc1k3* chloroplasts appeared to be morphologically similar to wild-type chloroplasts, but the thylakoid grana appeared slightly scattered, and there were very few or no visible starch granules. However, under HL treatment, *abc1k3* chloroplasts significantly differed from the wild-type chloroplasts, presenting large scattered grana and extensive vacuolation as well as an increase in plastoglobule size and number of plastoglobule clusters. Moreover, under HL no starch granules were observed in *abc1k3* chloroplasts (Fig. 2B).

In contrast, *vte1* chloroplasts did not significantly differ from the wild-type chloroplasts under normal light conditions. But a slight reduction of the number of starch granules and a reduction in the number and size of plastoglobules in *vte1* after HL treatment was

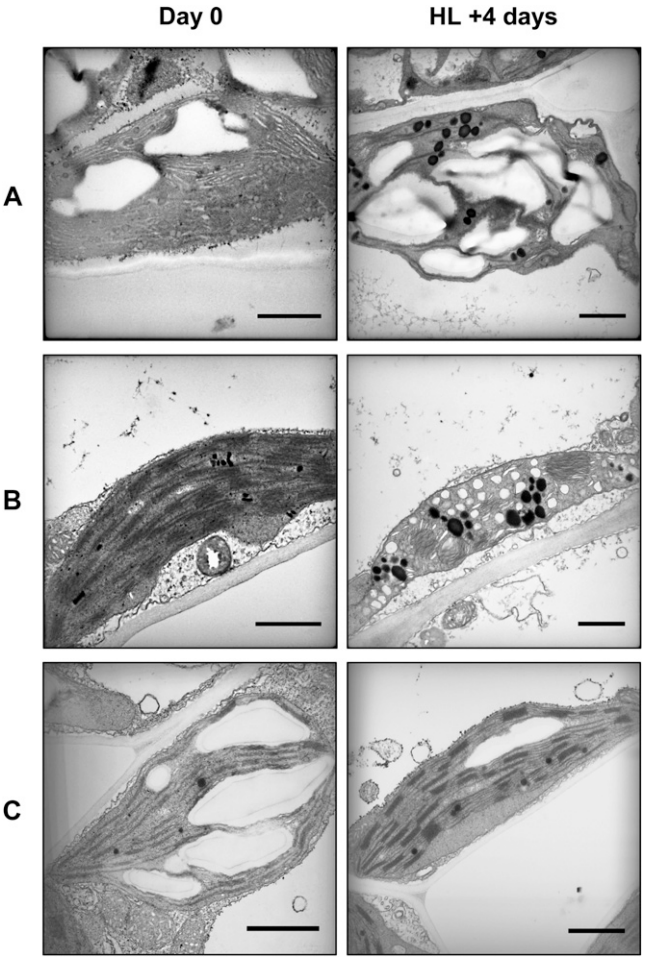

Figure 2. Changes in chloroplast ultrastructure observed under HL treatment. Transmission electron micrographs of leaves from wild-type (A), *abc1k3* (B), and *vte1* (C) plants exposed to normal light intensity (left, 150 μE m^{-2} s^{-1}) or to continuous HL (right, 500 μE m^{-2} s^{-1}) for 4 d. Black bars, 1 μm.

observed when compared with the wild type (Fig. 2C), as previously reported (Zbierzak et al., 2010).

ABC1K3 Has a Major Effect on Membrane Prenylquinone Composition

Ultra-high-pressure liquid chromatography coupled to atmospheric pressure chemical ionization-quadrupole time of flight mass spectrometry (UHPLC-APCI-QTOFMS), a powerful analytical technique for rapid and reliable lipid profiling of plant samples, was used to test whether the *abc1k3* mutant is affected in prenylquinone and/or carotenoid composition.

Total leaf extracts from 2-month-old Arabidopsis rosettes grown under normal light conditions or exposed to continuous HL stress for an increasing period of time (1, 2, and 7 d, respectively) were subjected to analysis, yielding more than 400 peaks in negative atmospheric pressure chemical ionization mode. The identified prenylquinones and carotenoids are presented in Supplemental Table S1.

Principal component analysis (PCA) was applied to highlight differences in the lipid composition of wild-type and *abc1k3* plants (Fig. 3, A and B). Both under normal light conditions and after HL exposure, wild-type and *abc1k3* samples clustered separately and differed significantly from *vte1*. Interestingly, the *abc1k3* cluster colocalized with the α-tocopherol (α-T) oxidative-derivate α-tocopherol quinone (α-TQ) but not with the other tocopherols, which were typical of wild-type samples. On the contrary, *vte1* samples colocalized with the xanthophyll lutein and the tocopherol precursor 2,3-dimethyl-5-phytyl-1,4-hydroquinone (DMPBQ).

A quantitative analysis of these prenylquinones and carotenoids was also performed to determine the variations in their content between the wild type, *abc1k3*, and *vte1* in response to HL exposure (Fig. 4). Similar α-, γ-, and δ-T levels were detected in the wild type and *abc1k3*, although a slightly slower accumulation rate was observed in *abc1k3* after prolonged HL exposure. The tocopherols were absent from *vte1*, as expected (Fig. 4, A, C, and D). However, under HL treatment, *abc1k3* accumulated significantly higher amounts of α-TQ, a tocopherol redox cycle intermediate generated in thylakoid membranes by spontaneous oxidation that is recycled in a VTE1-dependent manner (Fig. 4B). Strikingly, the levels of another VTE1 product, plastochromanol-8 (PC-8), were about 4-fold lower in *abc1k3* than in the wild type and did not significantly change after HL exposure (Fig. 4E). The *abc1k3* phenotype is not a phenocopy of *vte1*, because *vte1* completely lacks PC-8 (in addition to the absence of all tocopherols) but accumulates the precursor DMPBQ instead. DMPBQ was not detectable in *abc1k3* samples (data not shown), which contained all the tocopherols. Moreover, an accumulation of the xanthophyll lutein was observed in *vte1* both under normal growth conditions or after prolonged HL exposure, whereas its content in *abc1k3* was slightly lower than in the wild type under normal light, but increased after HL treatment (Fig. 4F). As previously observed by PCA of total lipidomics data, other molecules could be affected by the *abc1k3* mutation, yet no unambiguous identification could be achieved based on their mass-to-charge ratio. A complete list of all the detected molecules, as well as their relative abundance in the three tested plant lines and under different light conditions, is provided in Supplemental Table S2.

abc1k3 Mutants Have a Low VTE1 Content

Considering that the most relevant differences in prenylquinone composition of *abc1k3* plants depended on the enzymatic products of the VTE1, a possible variation in VTE1 content or subcellular localization was investigated by western-blot analysis. Besides, in order to investigate a potential effect of ABC1K3 on other plastoglobule proteins, antibodies raised against the two most abundant plastoglobule fibrillins (FBNs), FBN1a and FBN2, were used as well (Lundquist et al., 2012b). The thylakoid marker light-harvesting antenna type II chlorophyll a/b-binding protein (LHCb2) was used as control. Equal protein amounts of total chloroplast membrane fractions as well as purified chloroplast membrane subfractions corresponding to plastoglobules and thylakoids were extracted from plants grown under normal light conditions, then separated by SDS-PAGE, transferred to nitrocellulose, and probed using αVTE1, αFBN1a/b, αFBN2, and αLHCb2 antibodies (Fig. 5). VTE1 was detected in wild-type plastoglobules but was below the detection limit in *abc1k3*. As expected, VTE1 was not present in the knockout line *vte1*. Interestingly, the fibrillin FBN2 appeared to be much less abundant in *abc1k3* than in wild-type plastoglobules, while its content in *vte1* samples was only moderately lower than in wild-type samples. The use of αFBN1a antibodies for immunoblotting resulted in the detection of two distinct proteins with a predicted molecular mass slightly higher than 30 kD and corresponding to the two fibrillins FBN1a and FBN1b, as previously observed (Giacomelli et al., 2006). In *abc1k3* plastoglobules, both proteins were less abundant than in the wild type; *vte1* plastoglobules showed a similar intensity in the upper band (FBN1a), whereas that of the lower one (FBN1b) was reduced. With regard to the controls, no significant differences between the wild type, *abc1k3*, and *vte1* were observed for the thylakoid marker LHCb2.

VTE1 and *FBN1a* Are Overexpressed in *abc1k3* Plants

Both VTE1 and FBN1a protein levels were reduced in *abc1k3*. In order to determine whether the expression of the corresponding genes is affected or whether the reduction occurs at a posttranscriptional level, quantitative RT-PCR experiments were carried out for the two genes *VTE1* and *FBN1a* on total RNA extracted

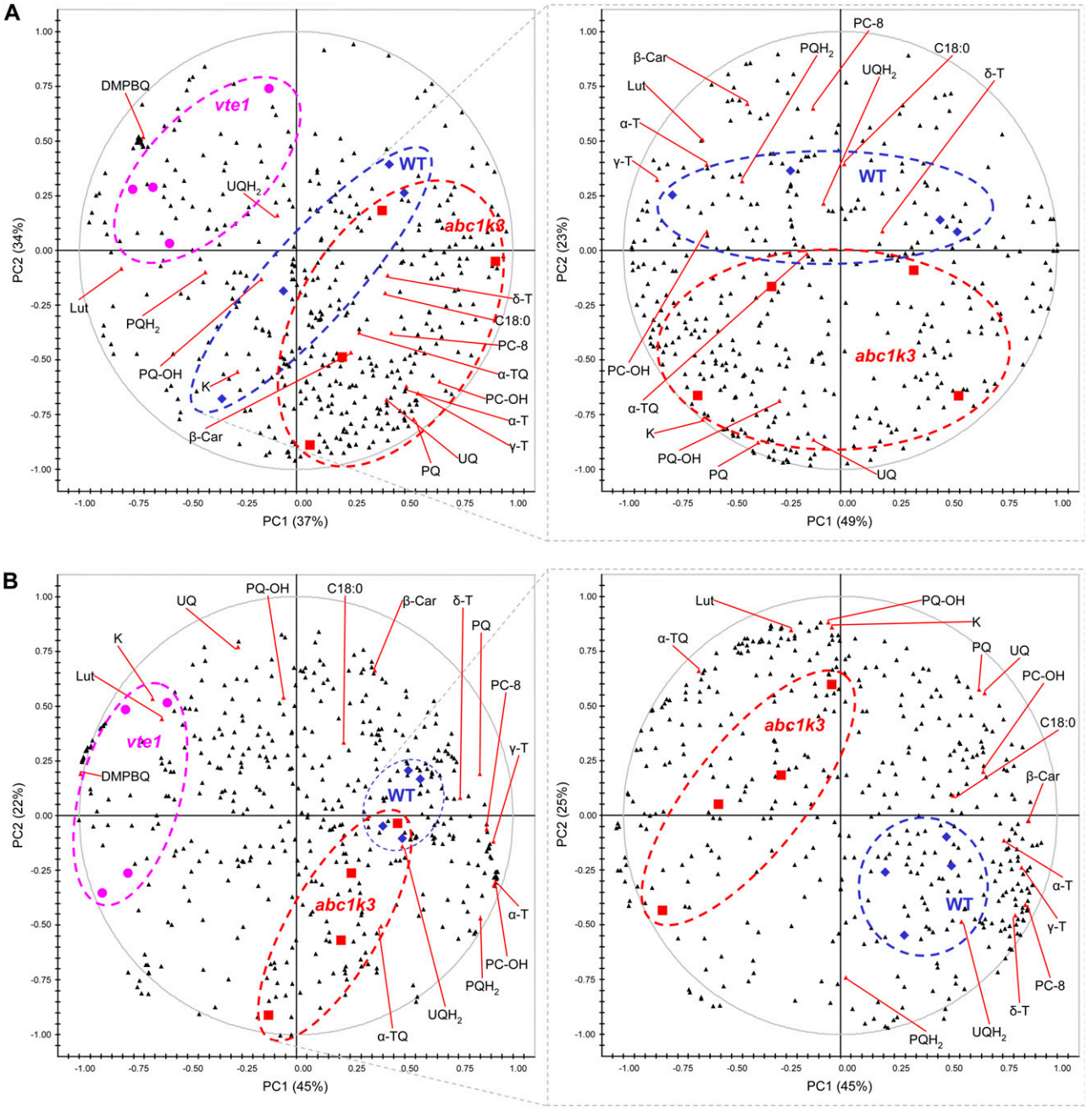

Figure 3. Biplots derived from an untargeted PCA showing differences between lipid profiles of different plant lines and after HL treatment. A, Plants grown under normal light conditions (150 μE m^{-2} s^{-1}). B, Plants exposed to continuous high light (500 μE m^{-2} s^{-1}) for 7 d. Inset on the right shows biplots from a PCA performed exclusively on wild-type and *abc1k3* data. Colored squares correspond to the observations (n = 4 for each plant line) and black triangles represent the variables. PC1 and PC2 are first and second principal components, respectively, with their percentage of explained variance. The identified prenylquinones and carotenoids are indicated (compare with Supplemental Table S1). WT. Wild type; Lut, lutein; β-Car, β-carotene; K, phylloquinone. For abbreviations see Supplemental Table S2.

from fresh wild-type, *abc1k3*, and *vte1* leaves. A significant increase (2.75-fold) in *VTE1* transcript levels was observed in *abc1k3* compared with wild-type plants, while only a weak, presumably background signal was detected in *vte1* (Fig. 6). At the same time, a significant increase in the expression of *FBN1a* was detected in both *abc1k3* and *vte1* mutants (1.5- and 2.2-fold more, respectively) when compared with the wild type (Fig. 6). Gene (co)expression was also investigated in silico using the ATTED-II database. *ABC1K3* and *VTE1* clustered together, and a strong correlation between the expression of the two genes was predicted

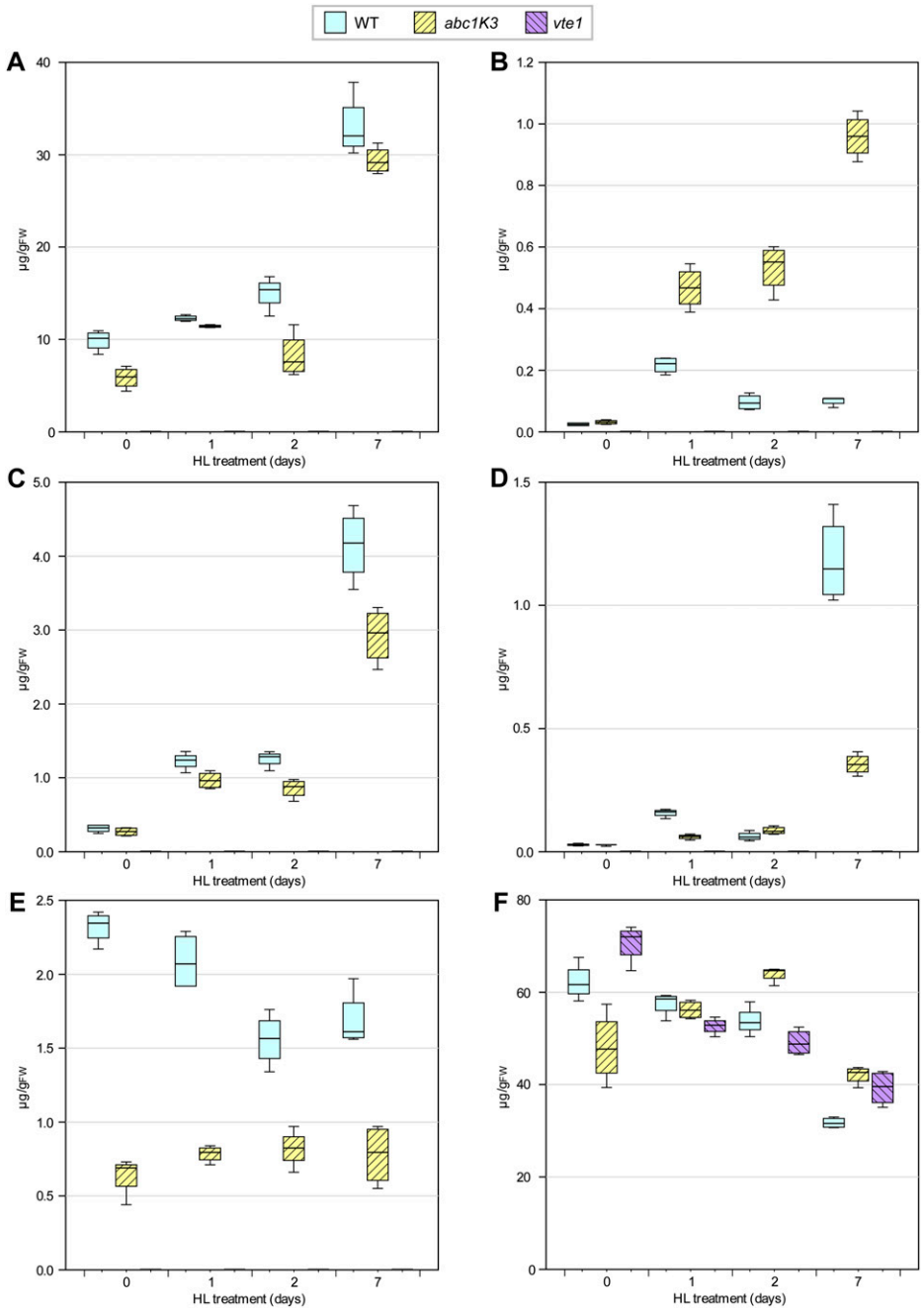

Figure 4. Comparison of the prenylquinone and carotenoid total leaf content. A, α-T. B, α-TQ. C, γ-T. D, δ-T. E, PC-8. F, Lutein. Plants grown under normal light conditions (day 0, 150 μE m^{-2} s^{-1}) were exposed to continuous high light (500 μE m^{-2} s^{-1}) for 1, 2, and 7 d, respectively. Data are from four biological replicates (±SD). WT, Wild type. [See online article for color version of this figure.]

under stress conditions, suggesting a functional interaction (Supplemental Fig. S3).

ABC1K3 Phosphorylates VTE1

ABC1K3 is a predicted kinase located in plastoglobules. Its targets are currently unknown, but our results suggest VTE1 is one of them. In order to test this, the mature form of the kinase was synthesized in a cell-free reticulocyte lysate (in vitro translation [IVT] mix) and used in phosphorylation reactions in the absence or presence of purified recombinant VTE1 and [γ-^{33}P]ATP. The reticulocyte lysate alone was used as negative control. The lysate contains all kinds of cellular proteins, including kinases as well as their substrates, and therefore a number of faint background bands can be observed (Fig. 7A). ^{33}P incorporation above the background levels (Fig. 7C) was detected in a protein band with an apparent molecular mass of about 45 kD in samples containing both the ABC1K3 IVT product and the purified VTE1, but it was absent both in the reticulocyte lysate alone and in the samples containing the lysate supplemented with ABC1K3 or VTE1 alone. The phosphoprotein had a predicted

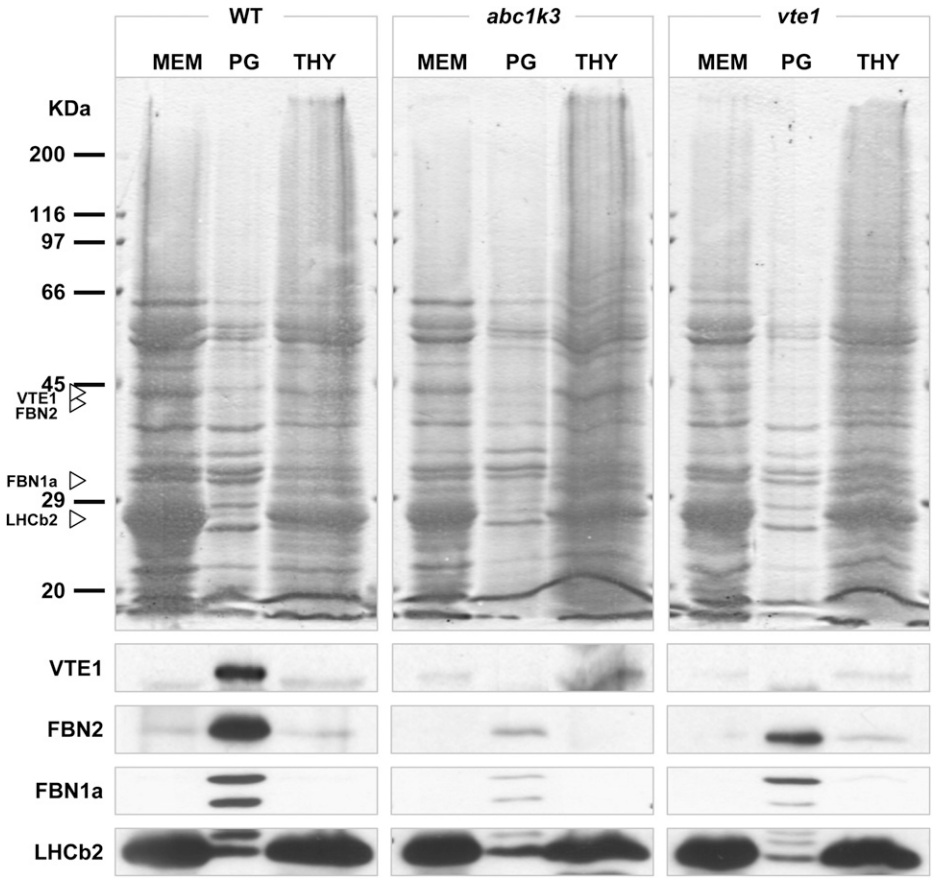

Figure 5. Western-blot analysis on purified chloroplast subfractions. Total proteins were extracted from total chloroplast membranes (MEM), plastoglobules (PG) and thylakoids (THY). Proteins were separated by SDS-PAGE, transferred to nitrocellulose membrane, and immunoblotted using the indicated antibodies raised against: the VTE1, the two most abundant plastoglobule fibrillins (FBN1a and FBN2, respectively) and the protein LHCb2. The positions of the detected proteins on the membrane are indicated by white triangles.

molecular mass that was consistent with that of VTE1 (43.5 kD; Fig. 7B). The absence of additional bands phosphorylated by ABC1K3 points to the specificity of the kinase reaction.

In parallel, protein identification was performed by western-blot analysis using antibodies raised against VTE1 or a His_6 tag on the recombinant kinase, which confirmed both ABC1K3 and VTE1 distribution in the samples and strongly supported VTE1 as the likely phosphoprotein (Fig. 7D).

DISCUSSION

ABC1K3 Affects Membrane Lipid Composition

To analyze the role of ABC1K3 in lipid metabolism we analyzed total leaf lipid extracts of wild-type and *abc1k3* and *vte1* mutant plants grown under both standard conditions and high light stress using UHPLC-APCI-QTOFMS. PCA highlighted differences in prenylquinone and carotenoid composition between the wild-type and mutant plant lines. Most strikingly, lower PC-8 and elevated α-TQ levels were already observed in *abc1k3* under normal growth conditions, while α-, γ- and δ-T contents remained similar to the wild type. PC-8 is a chromanol derivative of plastoquinone, and α-TQ is an intermediate of the recently discovered tocopherol redox cycle. Both PC-8 synthesis and α-TQ recycling require the VTE1 activity (Kobayashi and DellaPenna, 2008; Szymańska and Kruk, 2010) and were absent from the *vte1* mutant. Interestingly, though, and in contrast to *vte1*, no significant variations in the levels of DMPBQ were observed in the *abc1k3* mutant when compared with the wild type. These results demonstrate a very specific role of ABC1K3 in prenylquinone metabolism in regulating branches of VTE1 activity that may be located at the plastoglobule lipid droplets.

These results are consistent with the finding that VTE1 activity can be a limiting factor for PC-8 but not for tocopherol synthesis (Raclaru et al., 2006; Zbierzak et al., 2010). However, a comparative lipidomics analysis performed using the *vte1* mutant as a reference, lacking both PC-8 and tocopherols, showed that the *abc1k3* mutant does not simply correspond to an intermediate phenotype between wild-type and *vte1* plants but clusters separately, suggesting that molecules other than these prenylquinones may be affected as well.

ABC1K3 Affects VTE1 Activity and Plastoglobule Proteins

VTE1 levels were strongly reduced or absent in the total chloroplast membranes and subfractions derived from *abc1k3* and *vte1* mutants, respectively. However, the *VTE1* gene was transcribed at higher levels in *abc1k3* than in the wild type. These findings indicate

that VTE1 activity is posttranscriptionally downregulated in *abc1k3* mutants. Moreover, evidence is provided that the mature form of ABC1K3 phosphorylates VTE1 in vitro, suggesting that it is a target of the kinase. We hypothesize that phosphorylation by ABC1K3 stabilizes VTE1 at plastoglobules. It is conceivable that in the absence of ABC1K3-dependent phosphorylation VTE1 is degraded, explaining its lower content in *abc1k3* plastoglobules and the effect on the cellular levels of some of its metabolic products.

ABC1K3 Deletion Affects NPQ and Chloroplast Ultrastructure

When photosynthetic parameters and the response to HL intensity were measured, *abc1k3* did not significantly differ from the wild type, although it showed slightly lower NPQ levels under HL stress, possibly because of a slightly lower xanthophyll (lutein and zeaxanthin) content. Conversely, *vte1* had higher NPQ levels than the wild type after a short HL exposure because of the higher xanthophyll content, as previously reported (Havaux et al., 2005). However, after prolonged HL treatment, a reduction in both ETR and NPQ levels was observed in *vte1* plants, possibly because of photooxidative damage caused by the lack of PC-8 and tocopherols, which were instead present in *abc1k3*, although with PC-8 at a much lower concentration than in the wild type.

Moreover, the comparison of transmission electron micrographs of wild-type and *abc1k3* plants indicates a

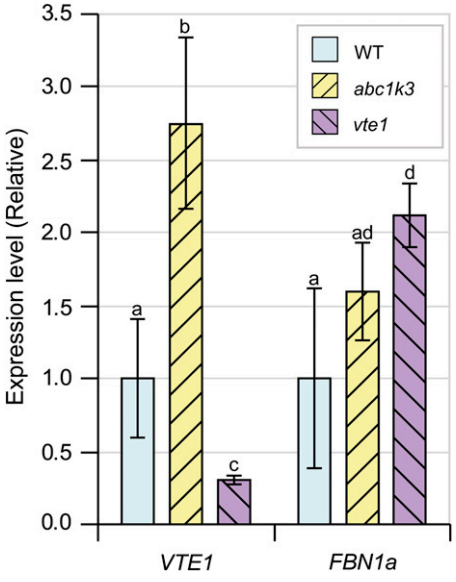

Figure 6. Changes in *VTE1* and *FBN1a* gene expression rate determined by real-time RT-PCR. Total RNA extracted from untreated leaves was used for PCR assays. *ACTIN2* expression levels were used for normalization. Significant differences between samples ($n = 3$ for each plant line) were determined by a one-way ANOVA. [See online article for color version of this figure.]

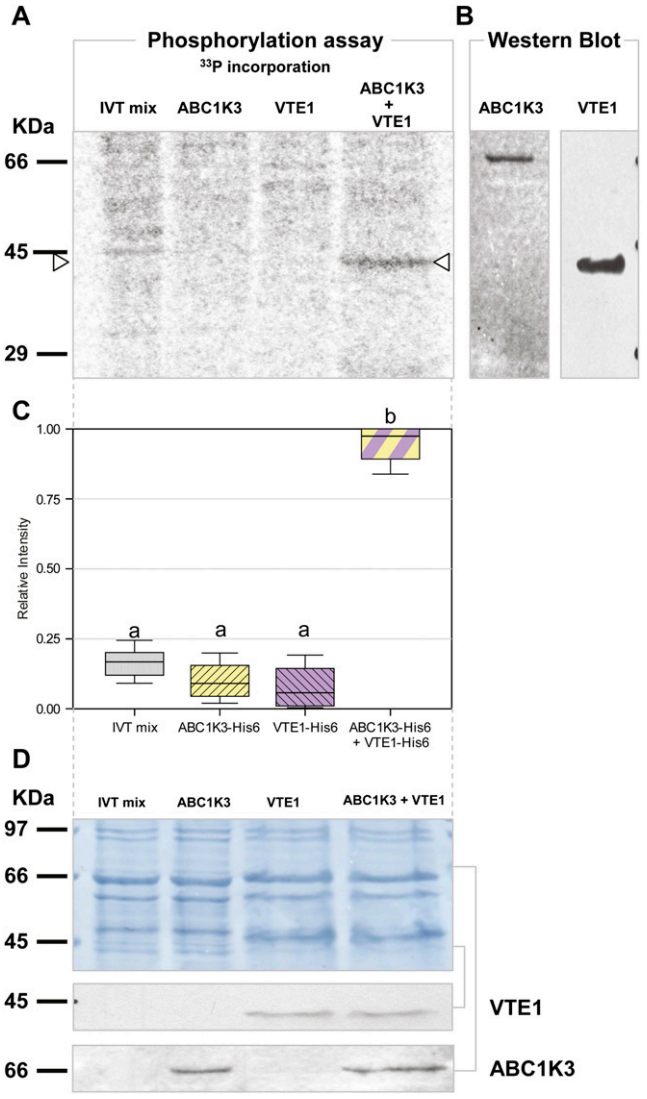

Figure 7. In vitro phosphorylation assays. A, VTE1 phosphorylation by ABC1K3. Recombinant ABC1K3-His_6 was synthesized in rabbit reticulocyte lysate (IVT mix) and used for in vitro phosphorylation reactions in the presence or absence of the purified recombinant VTE1-His_6. The IVT mix already contains multiple kinases and their phosphorylation targets and can thus serve as negative control. Reactions were supplemented with [γ-^{33}P]ATP, and ^{33}P incorporation in the samples was then determined by autoradiography. B, For comparison, the positions of ABC1K3-His_6 and VTE1-His_6 on the gel were determined by comigration with the two proteins independently detected by immunoblotting of separate SDS-PAGE gels. C, Phosphor Imager quantification of the relative intensity at the position of the white arrow (corresponding to VTE1-His_6). Significant differences between samples ($n = 4$ biological replicates) were determined by a one-way ANOVA. D, To validate the presence of the two proteins in the samples, phosphorylation reactions not supplemented with [γ-^{33}P]ATP were analyzed on separate SDS-PAGE gels, transferred on nitrocellulose membranes, and stained with Coomassie Blue (top); the presence of ABC1K3-His_6 and VTE1-His_6 was then determined by immunoblotting (bottom). [See online article for color version of this figure.]

possible effect of the mutation on chloroplast ultrastructure under HL conditions, which was not observed in plants lacking VTE1. In particular, *abc1k3* chloroplasts were characterized by large plastoglobule clusters, extensive vacuolation, and the absence of starch granules. These findings suggest that ABC1K3 may have targets other than VTE1 that are still unknown.

CONCLUSION

We demonstrate here that ABC1K3 affects the accumulation of VTE1-dependent metabolites, α-TQ and plastochromanol, most likely via phosphorylation of VTE1. Moreover, the evidence presented suggests that ABC1K3 acts on other targets that we have not yet identified. In conclusion, ABC1K3 may be involved in a far-ranging regulatory network regulating not only the synthesis of VTE1-derived prenylquinone products but also plastoglobule morphology, thylakoid integrity, and starch accumulation.

MATERIALS AND METHODS

Chemicals

The solvents used for plant lipid profiling were tetrahydrofuran (analytical grade, Normapur) from VWR and ethylacetate (analytical grade) from Acros Organics. UPLC/MS grade-grade MeOH and water from Biosolve were used for the UHPLC-APCI-QTOFMS analyses. Unless stated otherwise, all the other chemicals were purchased from Sigma-Aldrich.

Purified Standards for Lipidomics Analysis

α-T and γ-T and phylloquinone standards of HPLC grade (greater than or equal to 99.5%) were purchased from Sigma-Aldrich. δ-tocopherol (δ-T) standard was purchased from Supelco. α-TQ, plastoquinone-9 (PQ-9), and PC-8 standards were kindly provided by Dr. Jerzy Kruk (Jagiellonian University, Krakow, Poland). The oxidized and reduced PQ-9 standards were obtained as described in (Suhara et al., 2005) with slight changes (Martinis et al., 2011). Lutein and β-carotene standards were purchased from Extrasynthese.

Plant Material and Treatments

Wild-type Arabidopsis (*Arabidopsis thaliana*) plant always refers to var Columbia-0. *ABC1K3* disruption was tested using two T-DNA insertion lines, SALK_128696 and SAIL_918E10, both obtained from the Nottingham Arabidopsis Stock Centre (http://arabidopsis.info; Alonso et al., 2003). However, no phenotypical differences were observed between the two lines. For this reason, *abc1k3* always refers to SALK_128696 in this work. The mutant line for *VTE1* was a gift from Dr. P. Dörmann (Max Planck Institute, Golm, Germany) and was obtained by ethyl methanesulfonate mutagenesis as described in (Porfirova et al., 2002). Plants were grown on soil under standard growth conditions (150 $\mu E\ m^{-2}\ s^{-1}$, 8-h-light/21°C and 16-h-dark/18°C periods, 55% relative air humidity) according to the protocol described in (Hiltbrunner et al., 2001) with slight modifications.

HL treatments were performed on 1- or 2-month-old rosettes by exposure to continuous HL conditions (500 $\mu E\ m^{-2}\ s^{-1}$, 21°C, 55% relative air humidity); light was provided by 400-W metal halide lamps (Philips).

Mutant Genotyping

Rapid genomic DNA extraction from Arabidopsis leaves was performed as described in (Edwards et al., 1991). The predicted location of the T-DNA insertion in the two mutant lines SAIL_918E10 and SALK_128696 was at the 5′ end of the second exon and inside the third exon of *ABC1K3*, respectively. In order to select homozygous lines for T-DNA insertions, a three-primer PCR analysis was employed. The primer sets included a left and right genomic primer (LP and RP) designed on the regions flanking the predicted T-DNA insertion site (at the 5′ and 3′ ends of the T-DNA, respectively) and the left T-DNA border primer, designed on the inserted sequence. LBa1 of pBIN-pROK2 was used for SALK lines, while LB1 of pCSA110-pDAP101 was selected for SAIL lines. The left and right genomic primers were designed using the T-DNA Primer Design tool from the Salk Institute Genomic Analysis Laboratory. The T-DNA insertion line SAIL_918E10 was genotyped using the primer couples LPa (5′-GGGAGGAGGTAGTGACAAAGG-3′) and RPa (5′-AAGGTAATCGGGTGGACAGAG-3′), while for the SALK_128696 line the primers LPb (5′-TGTTGCTGTCAAAGTTCAACG-3′) and RPb (5′-CAAGCGTACTTTGAAGTTCCG-3′) were used. DNA extracted from wild-type Arabidopsis plants was used as reference. PCR reactions were then analyzed by agarose gel electrophoresis according to standard protocols (Sambrook and Russell, 2001).

Determination of the Photosynthetic Parameters

Fv/Fm, ETR, and NPQ were fluorometrically determined using a MINI-PAM Photosynthesis Yield Analyzer (Walz).

Arabidopsis Chloroplast Ultrastructural Analysis

Leaves from 4- to 5-week-old Arabidopsis rosettes were fixed overnight in 0.1 M phosphate buffer (pH 6.8) containing 4% (w/v) formaldehyde and 5% (w/v) glutaraldehyde, washed three times in 0.1 M phosphate buffer (pH 6.8) for 20 min, and postfixed for 2 h with 1% (w/v) osmium tetraoxide at 20°C. Samples were dehydrated in ethanol and acetone series and infiltrated overnight with a low-viscosity epoxy resin (Spurr; Polyscience). Leaf fragments were then placed in an appropriate mold, included in Spurr and heated for 4 h at 60°C to allow the resin to solidify. Ultrathin sections of 90 nm were prepared using an Ultracut-E microtome (Reichert-Jung) equipped with a diamond knife (Diatome), mounted on copper grids, and contrasted with a saturated uranyl acetate solution in 50% ethanol and with Reynolds' lead citrate according to Reynolds (1963). Ultrathin sections were observed with a Philips CM-100 electron microscope operating at 60 kV.

Arabidopsis Membrane Prenylquinone Profiling

Liquid chromatography-mass spectrometry analysis of leaf samples was performed as described in (Martinis et al., 2011) with the following modifications to allow the simultaneous separation and detection of prenylquinones and carotenoids: the initial MeOH percentage used for the chromatographic gradient was set to 80%, increased to 100% in 3 min, and maintained at 100% for 2 min. α-T, α-TQ, γ-T, δ-T, phylloquinone, PQ-9, PC-8, lutein, and β-carotene were quantified based on calibration curves built from standard compounds. Data were processed using MassLynx version 4.1 (Waters) and multivariate analysis was carried out using MarkerLynx XS (Waters). Variables were Pareto-scaled before applying PCA.

Chloroplast Fractionation and Western-Blot Analysis

Chloroplast membranes were extracted and fractionated as described in (Vidi et al., 2006) with slight modifications. To prevent proteolytic degradation and spontaneous dephosphorylation, 0.5% (v/v) protease inhibitor cocktail for plant cell extracts (P9599, Sigma) and 1% (v/v) phosphatase inhibitor cocktail 2 (P5726, Sigma) were added. Total proteins were extracted by chloroform-methanol precipitation (Wessel and Flügge, 1984), resuspended in an appropriate volume of sample buffer (50 mM Tris/HCl, pH 6.8, 0.1 M dithiothreitol, 2% [w/v] SDS, 0.1% [w/v] bromophenol blue, 10% [v/v] glycerol) and separated by SDS-PAGE. Blots were then probed with sera raised against the protein LHCb2 (kindly provided by Dr. K. Apel, Eidgenössische Technische Hochschule Zürich, Switzerland), the VTE1 (Kanwischer et al., 2005), and the two fibrillins FBN1a and FBN2 (Vidi et al., 2006).

Phosphorylation Assays

In order to test VTE1 as a possible target of ABC1K3, the coding sequence for the kinase without the transit peptide (in silico prediction performed using the TargetP 1.1 server; Emanuelsson et al., 2007) and including a C-terminal His_6 tag was cloned in the p0GWA expression vector, a derivate of pET22d (Merck)

described in Busso et al., 2005. The protein was then synthesized in vitro using the TNT Quick Coupled Transcription/Translation System (Promega) according to the manufacturer's recommendations. The expression vector VTE1-pQE31, encoding for the mature part of the VTE1 without the predicted signal peptide, was kindly provided by Dr. P. Dörmann (University of Bonn, Germany) and was used for protein expression, as previously described (Porfirova et al., 2002). VTE1 was then purified by affinity chromatography (Qiagen), mixed with the ABC1K3 IVT product in different combinations, and used in 100-μL in vitro phosphorylation reactions in a suitable phosphorylation buffer (50 mM HEPES/KOH, pH 7.5, 5 mM $MgCl_2$, 0.5 mM $MnCl_2$, 50 mM NaCl, 0.1 mM dithiothreitol) supplemented with 50 μM ATP and 2 μCi [γ-^{33}P] ATP. Reactions were incubated for 30 min at 25°C and under gentle shaking (300 rpm), then proteins were swiftly precipitated in chloroform-methanol (Wessel and Flugge, 1984) and resuspended in an appropriate volume of the previously described sample buffer. Proteins were separated by SDS-PAGE followed by Coomassie Blue staining and dried on two layers of Whatman filter paper. ^{33}P incorporation was detected after 3 d or more using a Personal FX Phosphorimager and analyzed using the QuantityOne software (both from Bio-Rad Laboratories). The identity of the radioactive band was confirmed by parallel western-blot analysis using antibodies raised against VTE1 (see previous section).

Gene Expression

Total RNAs were purified from Arabidopsis leaves using the RNeasy Plant Mini Kit (Qiagen), according to the supplier's recommendations, and DNase treatment was performed on column using the RNase-free DNase set (Qiagen). Complementary DNAs were then prepared using the GoScript Reverse Transcriptase kit (Promega) in the presence of RNasin RNase inhibitors (Promega), and stored at −20°C. For quantitative PCR, the housekeeping gene *ACTIN2* was used as reference and amplified using the primer couple act2-S (5′-TGGAATCCACGAGACAACCTA-3′) and act2-AS (5′-TTCTGTGAACGATTCCTGGAC-3′). For the analysis of *ABC1K3* expression level in the mutant, the primer couple ABC1K3_q_F (5′-GCTTTGATCCTGCTATTTTG-3′) and ABC1K3_q_R (5′-GTGGCTCGAAGAAGTTGTTG-3′) were used. For the analysis of *VTE1* and *FBN1a* expression, the following primers were designed: VTE1_q_F (5′-GTGCTCCTACCACAGAAGTT-3′), VTE1_q_R (5′-TATCTCCACTGCTGCCATTG-3′), FBN1a_q_F (5′-CAAACCATTGATTCCGATAG-3′), and FBN1a_q_R (5′-AGTCCCTATAACACCTTGCT-3′). Real-time PCR reactions ($n = 3$) were assembled in a final volume of 20 μL using the ABsolute qPCR SYBR Green mix (ABgene), 10 μM of both 5′ and 3′ primers, and adjusted amounts of complementary DNA diluted 40 times in distilled, deionized water. The PCR program was as follows: 15 min, 95°C (thermo-start); 45× (20 s, 95°C; 30 s, 55°C; 45 s, 72°C); and 1 min, 55°C; and was followed by an 80-step dissociation (55°C to 95°C). SYBR Green emission was detected in real time in an iQ5 Optical System (Bio-Rad Laboratories), and data were treated using the included software. A one-way ANOVA was conducted on the obtained data. When a significant difference was detected, a Tukey's honestly significant difference mean-separation test was applied at a significance level of $P < 0.05$.

Gene coexpression was determined in silico using the ATTED-II 6.0 database (Obayashi et al., 2011).

Sequence data from this article can be found in the EMBL/GenBank data libraries under accession numbers AEE36271.1 (*ABC1K3*, At1g79600.1), AEE86116.1 (*VTE1*, At4g32770.1), AEE82363.1 (*FBN1a*, At4g04020.1), AEC09113.1 (*FBN2*, At2g35490.1), AEC05893.1 (*LHCB2*, At2g05070.1), and AEE76147.1 (*ACTIN2*, At3g18780.1).

Supplemental Data

The following materials are available in the online version of this article.

Supplemental Figure S1. Isolation of *ABC1K3* T-DNA insertion mutants.

Supplemental Figure S2. Comparison between wild-type plants and the two *abc1k3* T-DNA insertion mutant alleles SALK_128696 and SAIL_918E10.

Supplemental Figure S3. Predicted *ABC1K3* coexpressed gene network.

Supplemental Table S1. List of the molecules identified from UHPLC-APCI-QTOFMS data acquired in negative ionization mode.

Supplemental Table S2. List of all the molecular markers detected by UHPLC-APCI-QTOFMS lipid profiling and relative abundance in analyzed samples.

ACKNOWLEDGMENTS

We thank Jerzy Kruk from Jagiellonian University for kindly providing purified α-TQ, PQ-9 and PC-8 standards, and Claus Wedekind from the University of Lausanne for providing carotenoid standards. J.M. performed the research and analyzed the data. G.G. conducted the UHPLC-APCI-QTOFMS measurements. S.V. carried out the purification of the VTE1 used in the phosphorylation assays. J.M. and F.K. conceived the study and wrote the manuscript. All authors read, commented, and approved the final manuscript.

LITERATURE CITED

Alonso JM, Stepanova AN, Leisse TJ, Kim CJ, Chen HM, Shinn P, Stevenson DK, Zimmerman J, Barajas P, Cheuk R, et al (2003) Genome-wide insertional mutagenesis of Arabidopsis thaliana. Science **301:** 653–657

Bousquet I, Dujardin G, Slonimski PP (1991) ABC1, a novel yeast nuclear gene has a dual function in mitochondria: it suppresses a cytochrome b mRNA translation defect and is essential for the electron transfer in the bc 1 complex. EMBO J **10:** 2023–2031

Bouvier F, Rahier A, Camara B (2005) Biogenesis, molecular regulation and function of plant isoprenoids. Prog Lipid Res **44:** 357–429

Boyd JS, Mittelmeier TM, Lamb MR, Dieckmann CL (2011) Thioredoxin-family protein EYE2 and Ser/Thr kinase EYE3 play interdependent roles in eyespot assembly. Mol Biol Cell **22:** 1421–1429

Brasseur G, Tron G, Dujardin G, Slonimski PP, Brivet-Chevillotte P (1997) The nuclear *ABC1* gene is essential for the correct conformation and functioning of the cytochrome bc_1 complex and the neighbouring complexes II and IV in the mitochondrial respiratory chain. Eur J Biochem **246:** 103–111

Bréhélin C, Kessler F (2008) The plastoglobule: a bag full of lipid biochemistry tricks. Photochem Photobiol **84:** 1388–1394

Derurère J, Römer S, d'Harlingue A, Backhaus RA, Kuntz M, Camara B (1994) Fibril assembly and carotenoid overaccumulation in chromoplasts: a model for supramolecular lipoprotein structures. Plant Cell **6:** 119–133

Do TQ, Hsu AY, Jonassen T, Lee PT, Clarke CF (2001) A defect in coenzyme Q biosynthesis is responsible for the respiratory deficiency in *Saccharomyces cerevisiae abc1* mutants. J Biol Chem **276:** 18161–18168

Edwards K, Johnstone C, Thompson C (1991) A simple and rapid method for the preparation of plant genomic DNA for PCR analysis. Nucleic Acids Res **19:** 1349

Emanuelsson O, Brunak S, von Heijne G, Nielsen H (2007) Locating proteins in the cell using TargetP, SignalP and related tools. Nat Protoc **2:** 953–971

Giacomelli L, Rudella A, van Wijk KJ (2006) High light response of the thylakoid proteome in Arabidopsis wild type and the ascorbate-deficient mutant *vtc2-2*. A comparative proteomics study. Plant Physiol **141:** 685–701

Havaux M, Eymery F, Porfirova S, Rey P, Dörmann P (2005) Vitamin E protects against photoinhibition and photooxidative stress in *Arabidopsis thaliana.* Plant Cell **17:** 3451–3469

Hiltbrunner A, Bauer J, Vidi PA, Infanger S, Weibel P, Hohwy M, Kessler F (2001) Targeting of an abundant cytosolic form of the protein import receptor at Toc159 to the outer chloroplast membrane. J Cell Biol **154:** 309–316

Jasinski M, Sudre D, Schansker G, Schellenberg M, Constant S, Martinoia E, Bovet L (2008) AtOSA1, a member of the Abc1-like family, as a new factor in cadmium and oxidative stress response. Plant Physiol **147:** 719–731

Kanwischer M, Porfirova S, Bergmüller E, Dörmann P (2005) Alterations in tocopherol cyclase activity in transgenic and mutant plants of Arabidopsis affect tocopherol content, tocopherol composition, and oxidative stress. Plant Physiol **137:** 713–723

Knoell HE (1981) Stand-by position of the dioxygen-dependent ubiquinone-8 synthesis apparatus in anaerobically grown *Escherichia coli* k-12. FEMS Microbiol Lett **10:** 59–62

Kobayashi N, DellaPenna D (2008) Tocopherol metabolism, oxidation and recycling under high light stress in *Arabidopsis*. Plant J **55:** 607–618

Kreimer G (2009) The green algal eyespot apparatus: a primordial visual system and more? Curr Genet **55:** 19–43

Leonard CJ, Aravind L, Koonin EV (1998) Novel families of putative protein kinases in bacteria and archaea: evolution of the "eukaryotic" protein kinase superfamily. Genome Res **8:** 1038–1047

Lundquist PK, Davis JI, van Wijk KJ (2012a) ABC1K atypical kinases in plants: filling the organellar kinase void. Trends Plant Sci **9:** 546–555

Lundquist PK, Poliakov A, Bhuiyan NH, Zybailov B, Sun Q, van Wijk KJ (2012b) The functional network of the Arabidopsis plastoglobule proteome based on quantitative proteomics and genome-wide coexpression analysis. Plant Physiol **158:** 1172–1192

Martinis J, Kessler F, Glauser G (2011) A novel method for prenylquinone profiling in plant tissues by ultra-high pressure liquid chromatography-mass spectrometry. Plant Methods **7:** 23

Mène-Saffrané L, DellaPenna D (2010) Biosynthesis, regulation and functions of tocochromanols in plants. Plant Physiol Biochem **48:** 301–309

Mollet J, Delahodde A, Serre V, Chretien D, Schlemmer D, Lombes A, Boddaert N, Desguerre I, de Lonlay P, de Baulny HO, et al (2008) CABC1 gene mutations cause ubiquinone deficiency with cerebellar ataxia and seizures. Am J Hum Genet **82:** 623–630

Obayashi T, Nishida K, Kasahara K, Kinoshita K (2011) ATTED-II updates: condition-specific gene coexpression to extend coexpression analyses and applications to a broad range of flowering plants. Plant Cell Physiol **52:** 213–219

Poon WW, Davis DE, Ha HT, Jonassen T, Rather PN, Clarke CF (2000) Identification of *Escherichia coli ubiB*, a gene required for the first monooxygenase step in ubiquinone biosynthesis. J Bacteriol **182:** 5139–5146

Porfirova S, Bergmuller E, Tropf S, Lemke R, Dormann P (2002) Isolation of an *Arabidopsis* mutant lacking vitamin E and identification of a cyclase essential for all tocopherol biosynthesis. Proc Natl Acad Sci USA **99:** 12495–12500

Raclaru M, Gruber J, Kumar R, Sadre R, Luhs W, Zarhloul MK, Friedt W, Frentzen M, Weier D (2006) Increase of the tocochromanol content in transgenic *Brassica napus* seeds by overexpression of key enzymes involved in prenylquinone biosynthesis. Mol Breed **18:** 93–107

Reynolds ES (1963) The use of lead citrate at high pH as an electron-opaque stain in electron microscopy. J Cell Biol **17:** 208–212

Sambrook J, Russell DW (2001) Molecular Cloning: A Laboratory Manual. Cold Spring Harbor Laboratory Press, Cold Spring Harbor, New York

Steinmuller D, Tevini M (1985) Composition and function of plastoglobuli. 1. Isolation and purification from chloroplasts and chromoplasts. Planta **163:** 201–207

Suhara Y, Kamao M, Tsugawa N, Okano T (2005) Method for the determination of vitamin K homologues in human plasma using high-performance liquid chromatography-tandem mass spectrometry. Anal Chem **77:** 757–763

Szymańska R, Kruk J (2010) Plastoquinol is the main prenyllipid synthesized during acclimation to high light conditions in Arabidopsis and is converted to plastochromanol by tocopherol cyclase. Plant Cell Physiol **51:** 537–545

Vidi PA, Kanwischer M, Baginsky S, Austin JR, Csucs G, Dörmann P, Kessler F, Bréhélin C (2006) Tocopherol cyclase (VTE1) localization and vitamin E accumulation in chloroplast plastoglobule lipoprotein particles. J Biol Chem **281:** 11225–11234

Wessel D, Flügge UI (1984) A method for the quantitative recovery of protein in dilute solution in the presence of detergents and lipids. Anal Biochem **138:** 141–143

Xie LX, Hsieh EJ, Watanabe S, Allan CM, Chen JY, Tran UC, Clarke CF (2011) Expression of the human atypical kinase ADCK3 rescues coenzyme Q biosynthesis and phosphorylation of Coq polypeptides in yeast *coq8* mutants. Biochim Biophys Acta **1811:** 348–360

Yang S, Zeng X, Li T, Liu M, Zhang S, Gao S, Wang Y, Peng C, Li L, Yang C (2012) *AtACDO1*, an ABC1-like kinase gene, is involved in chlorophyll degradation and the response to photooxidative stress in *Arabidopsis*. J Exp Bot 63: 3959–3973

Ytterberg AJ, Peltier JB, van Wijk KJ (2006) Protein profiling of plastoglobules in chloroplasts and chromoplasts. A surprising site for differential accumulation of metabolic enzymes. Plant Physiol **140:** 984–997

Zbierzak AM, Kanwischer M, Wille C, Vidi PA, Giavalisco P, Lohmann A, Briesen I, Porfirova S, Bréhélin C, Kessler F, et al (2010) Intersection of the tocopherol and plastoquinol metabolic pathways at the plastoglobule. Biochem J **425:** 389–399